



Science Arts & Métiers (SAM)

is an open access repository that collects the work of Arts et Métiers Institute of Technology researchers and makes it freely available over the web where possible.

This is an author-deposited version published in: <https://sam.ensam.eu>
Handle ID: <http://hdl.handle.net/10985/24624>

To cite this version :

Arpita CHATTERJEE, Soumyadeep SEN, Subhodeep PAUL, PALLAB ROY, Asiful SEIKH, Ibrahim ALNASER, Kalyan DAS, Goutam SUTRADHAR, Manojit GHOSH - Fabrication and Characterization of SiC-reinforced Aluminium Matrix Composite for Brake Pad Applications - Metals - 2023




Any correspondence concerning this service should be sent to the repository

Administrator : scienceouverte@ensam.eu



Article

Fabrication and Characterization of SiC-reinforced Aluminium Matrix Composite for Brake Pad Applications

Arpita Chatterjee ^{1,2}, Soumyadeep Sen ³, Subhodeep Paul ¹, Pallab Roy ⁴, Asiful H. Seikh ⁵ , Ibrahim A. Alnaser ⁵ , Kalyan Das ⁶ , Goutam Sutradhar ² and Manojit Ghosh ^{3,*}

- ¹ Department of Mechanical Engineering, Dr. Sudhir Chandra Sur Institute of Technology & Sports Complex, Kolkata 700074, West Bengal, India
- ² Department of Mechanical Engineering, National Institute of Technology, Imphal 795004, Manipur, India
- ³ Department of Metallurgy and Materials Engineering, Indian Institute of Engineering Science and Technology, Shibpur, Howrah 711103, West Bengal, India
- ⁴ Department of Mechanical Engineering, Budge Budge Institute of Technology, Kolkata 700137, West Bengal, India
- ⁵ Mechanical Engineering Department, College of Engineering, King Saud University, Riyadh 11421, Saudi Arabia
- ⁶ Arts et Metiers Institute of Technology, University of Bordeaux, CNRS, Bordeaux INP, INRAE, I2M Bordeaux, F-33400 Talence, France
- * Correspondence: mghosh.metal@faculty.iiests.ac.in

Abstract: The wear debris from conventional brake pads is a growing source of environmental contamination that often leads to life-threatening diseases for human beings. Though the emerging organic brake pads show potential to serve as an eco-friendly alternative, their mechanical and tribological properties are not adequate to withstand the demands of high-wear resistance of a functioning braking system under regular use. Metal matrix composites have served as an optimal solution with minimal environmental pollution and appreciable physical properties. Owing to the popularity of aluminium metal matrix composites, the present study is based on the fabrication and characterization of SiC-reinforced LM6 alloy through stir casting methodologies for evaluating its worthiness in application as a brake pad material. Microstructural, compositional, and phase characterizations were executed through optical micrography, X-ray diffraction, and energy-dispersive X-ray spectroscopy analysis. Although mechanical properties were evaluated through surface hardness investigation, parallel thermal properties were estimated through thermal conductivity evaluation. Finally, the execution of tribological analysis and precise microstructural observations of wear track at ambient and elevated temperatures helped in establishing the datum that the fabricated metal matrix composite (MMC) is a reliable brake pad material alternative.

Keywords: metal matrix composite; stir casting; brake pad; surface hardness; tribological analysis; SiC reinforcements



Citation: Chatterjee, A.; Sen, S.; Paul, S.; Roy, P.; Seikh, A.H.; Alnaser, I.A.; Das, K.; Sutradhar, G.; Ghosh, M. Fabrication and Characterization of SiC-reinforced Aluminium Matrix Composite for Brake Pad Applications. *Metals* **2023**, *13*, 584. <https://doi.org/10.3390/met13030584>

Academic Editors: Gunter Gerbeth and Slobodan Mitrovic

Received: 23 January 2023

Revised: 10 February 2023

Accepted: 5 March 2023

Published: 13 March 2023



Copyright: © 2023 by the authors. Licensee MDPI, Basel, Switzerland. This article is an open access article distributed under the terms and conditions of the Creative Commons Attribution (CC BY) license (<https://creativecommons.org/licenses/by/4.0/>).

1. Introduction

The braking system of a functioning automobile usually consists of a rotating “disc” and a static component called the “pad” responsible for ensuring the efficient deceleration of the vehicle through the effect of frictional contact between the disc–pad interface. It is necessary to consider that the conventionally fabricated brake pads rely on the strength and wear resistance of metallic/asbestos materials as constituents of a potent braking system. However, as expected, the constant frictional effects of a braking mechanism lead to particulate exhaust emission that results in the contamination of the environment with elements like Fe, Cu, Si, Ba, K, Ti, and so on.

These harmful particulate emissions are responsible for potentially exaggerating respiratory organ and optical nerve infections and causing life-threatening diseases such as

cancer and kidney and liver failures [1]. Furthermore, humans are not the only species suffering from the hazardous effects of exhaust emissions, since the phytotoxicity of these wear emissions also adversely affects the plant kingdom through loss of plasma membrane [2]. Understandably, the researchers are looking to fabricate novel materials intended to serve as an alternative to the conventionally used brake pad material. Several attempts have been made to suggest organic materials as a potential candidate for this purpose. Asbestos-free brake pads composed of banana peels have been suggested, as it displayed promising performance to serve as a replacement [3]. Another study based on the estimation of frictional behaviour of a brake pad material fabricated from waste tire dust showed prominent displays of being a reliable alternative [4]. Shells of cocoa beans [5] and bio-composites [6] also proved to be effective in terms of their wear-resisting abilities in several studies. Bahari et. al. [7] investigated the hardness and impact resistance of rice husk dust-composed automotive brake pad. The hardness resistance of automotive brake pad variegated with 30% RHD was higher than 10%, whereas the impact resistance of an automotive brake pad with 30% 80-mesh size of RHD was considerably greater than 100-mesh, owing to the ability of larger RHD to contest high-impact loading. Compared to the commercial brake pad, the RHD-composed brake pad provided superior hardness. The brake pad composed with finer and a lesser percentage of RHD demonstrated greater friction coefficient.

Nevertheless, the mechanical and tribological performances from completely organic material-based brake pads cannot be expected to be at par with the hardness and wear resistance of metal matrix composites. Owing to their high strength-to-weight ratio and excellent tribological behaviour, aluminum metal matrix composites can be considered to be one of the most suitable candidates for manufacturing brake pad material. However, extensive investigations of the mechanical and tribological properties of these composites are necessary before considering them as suitable candidates to serve as an alternative brake pad material, which can be somewhat referred to, from the vast quantity of literature available. K. Komai et al. [8] investigated the tensile and fatigue behaviour of SiC whisker-reinforced Al 7075 alloy composite material in normal and water environments and established a comparative results discussion and behavioural changes of the reinforced and non-reinforced materials. The specimen underwent a tensile test and fatigue test, and the roughness of the crack part along with the influence of an aqueous environment were determined using SEM images; the results showed that the reinforced composite has better tensile and fatigue strength properties than non-reinforced Al 7075. However, it has been found that in water, corrosion leads to cracks with weaker fatigue strength than in ambient condition.

Daoud et. al. [9] studied the influence of varying load and speed range on wear and friction behaviour of the sand cast brake rotor of A359-20 vol% SiC particle composites rotating disc sliding against the automobile friction material pin, and they compared the behaviour against a commercial cast iron brake rotor. They observed that for the 30 to 50 N load, the rise of the wear rate of the composite disc decreased, whereas from 50 to 100 N, it increased. On the other hand, the wear rate decreased with the rise in sliding speed of 3–9 m/s at all levels of load application, and in all cases, it was higher compared to that of the cast iron. At all ranges of sliding speeds, the friction coefficient of the disc decreased with load. The wear rate of the friction material demonstrated better wear resistance at greater speeds. The friction coefficient of the composite was found to be higher than that of the cast iron at all test conditions. The composite disc exhibited steady and greater friction coefficient in comparison to cast iron, which is crucial for brake rotor application. Compared to cast iron, the A359-20 vol% SiC brake rotor displayed better wear resistance, greater thermal conductivity, lighter weight, and constant friction coefficient, which are essential to reduce braking distance and noise.

WD Fei et al. [10] examined the effect of thermal residual stress creeping on the strength properties of SiC whisker-reinforced Al metal matrix composite. The Al composite was fabricated using the squeeze casting technique, then underwent a tensile test. Later, the material was treated with thermal residual stress creeping treatment and again tested

for the tensile strength. The results showed that the tensile strength properties of the material increase after TRSC treatment and the UTS of the material can go up to 330 MPa after TRSC for the Sic whisker-reinforced composite. S. Ghanaraja et al. [11] reinforced a powder mixture of aluminium and manganese in the ratio of 1:7 by weight that was mixed for 450, 600, and 750 min into molten aluminium for the synthesis of Al nano composite to determine the effects of particle size and tensile properties. The SEM and XRD images reflected that the porosity of the composite increases with increasing milled powder mixture; however, the tensile test proved that the nano-composite improved strain hardening and also increased the yield strength and ultimate strength compared to the base alloy.

M. Palanivendhan et al. [12] reinforced Al 6262 alloy with bagasse ash and fabricated the Al metal matrix composite using the stir casting method to determine its mechanical and tribological behaviour and check whether it can be a possible material used in the automobile and aircraft industry. The fabricated composite then underwent a tensile test, Vickers hardness test, and pin-on-disc tribometer test for frictional wear properties. The test results show that the mechanical and frictional properties depend on dispersion of reinforcement in the matrix, and proper dispersion increases the mechanical properties along with improving wear resistance. However, Faiz Ahmad et al. [13] fabricated an alumina-reinforced Al matrix composite to determine its frictional behaviour and wear behaviour and brake disc material when casted using the squeeze casting technique with 30% alumina by volume. The wear test was carried out at 25, 50, 75, and 100 N load, and the result showed that the wear rate increased with load, whereas the COF is consistent till 50N, then decreased with an increase in load.

Mohammad Mohsin Khan et al. [14] made an effort to examine the mechanical and erosive wear behaviour of SiC and fly ash reinforced ADC-12 Al alloy fabricated through liquid metallurgy. The fabricated composite then underwent microstructure, mechanical characterisation, and also erosive wear. The microstructure showed a uniform distribution of particles in the matrix, whereas the mechanical properties were found to decrease upon the addition of SiC particles, and the opposite scenario was true for fly ash. However, the material showed better wear resistance. Similarly, N. Mahaviradhan et al. [15] fabricated an aluminium hybrid matrix composite by reinforcing LM16 aluminium alloy with SiC in 0.5 and 10% by weight ratio and Nickel coated graphite 2% by weight using the stir casting method to understand the tribological behaviour of the aluminium method matrix at a high temperature. The experiment was performed on a pin-on-disc tribometer, and the results concluded that load is the prominent factor for wear, and the composite element has lesser frictional coefficient than the parent alloy at higher temperatures due to Ni-Gr and SiC reinforcement.

G. Karthikeyan et al. [16] fabricated an aluminium matrix composite with LM6 aluminium alloy as a base matrix and ZrO_2 as reinforcement in varying weight percentages varying from 0–12% using the stir casting technique. The sample specimens then underwent microstructure analysis as well as mechanical and thermal analysis, and the results concluded that the composite with 12% by weight ZrO_2 had the maximum tensile and compressive strength of 209 MPa and 218 MPa, respectively, along with better heat transfer rate, efficiency, and effectiveness, which made it the ideal fin material, among others. Samuel Olukayode et al. [17] investigated the microstructural and mechanical behaviour of heat-treated TiFe and SiC-reinforced LM6 aluminium alloy fabricated by stir casting technique and heat treated under T6 condition. The composite was then tested for microstructure and mechanical and frictional properties, and the results showed that the heat treatment improves the mechanical and tribological properties. Moreover, a transformation from the acircular structure to a globular shape was found due to the heat treatment in micrographs.

S. Madhavarao et al. [18] investigated the dry sliding wear behaviour of Al-7075 reinforced with SiC by conducting experiments following Taguchi's L9 method on pin-on-disc tribometer and fabricated using the stir casting technique to determine the tribological properties. The experimental results concluded that the sliding distance has the highest

influence on wear rate, whereas applied load has the highest influence on the coefficient of friction. It was also found that increasing the weight percentage of SiC increases wear resistance. Kalthapure et al. [19], in an attempt to realize the importance of the selection of materials to make different elements of brake systems and determine in what way worn particles affect the environment and humans, applied L25 orthogonal array with arranged control factors in the design of the experiment. In dry sliding conditions, they performed wear tests on the pin-on-disc tribometer with 25–125 N load, 300–1500 rpm sliding speeds, and 40–120 mm track diameter using the Taguchi method. The ANOVA results revealed that on the wear rate of the pad friction material, applied load factor is the most significant (48.27%), followed by track diameter (25%) and sliding speed (19.23%). The computed and experimental wear rates differed by only 1.93%. The measured values were 95% within the confidence level, according to the confirmation test results.

Although a large amount of existing literature indicates the suitability of aluminium matrix composites, especially with SiC reinforcements, for applications that demand high surface hardness and wear resistance, the application of LM6 Aluminium alloy matrix reinforced with SiC particulates fabricated using the stir casting technique has not yet been studied thoroughly. The present study not only focusses on estimating the hardness and thermal and tribological behaviour of the SiC-reinforced LM6 matrix composites at room temperature but also aims at evaluating these properties at elevated temperatures to simulate real-life conditions where the generation of heat through frictional action of the braking system is inevitable. Thus, the results obtained could justify the worth of SiC-reinforced LM6 matrix composites fabricated through stir casting in real-life applications, particularly as brake pad material. Hence, the objective of the present study can be considered an attempt to establish the prominence of the fabricated MMC as an alternative brake pad material that provides an optimized performance with lesser contaminant emission as compared to asbestos-based brake pads as well as improved performance in contrast to the newly developed organic brake pad materials.

2. Materials and methods

2.1. Materials

An extensive literature survey was conducted to determine the constituent materials to fabricate the metal matrix composite (MMC) for its implementation as brake pad material. Although a large amount of evidence obtained from innumerable studies [20] suggest aluminium alloys as the most suitable base matrix for producing an MMC with appreciable strength-to-weight ratios, making it perfect for automobile applications [21], the correct choice of aluminium alloy is expected to play an influential role. Apart from previous studies achieving promising results in terms of mechanical strength [22] and light weight appreciable wear resistance [23–25], the LM6 aluminium alloy was deemed as the perfect candidate for manufacturing a novel brake pad material, primarily owing to its exceptional fluidity [26], which makes it a top choice for producing MMC using the casting technique.

Though aluminum and aluminum alloys are more expensive than standard materials, it is equally true that a decrease in price can be achieved by increasing their quantities in production and additionally by enlarging the area of their usage. It has been established by research that globally, 4.1 and 4.4 million kilograms of MMC were used, respectively, in 2007 and 2008 [27]. It was projected that for 2013, the demand would be 5.9 million kilograms with an annual increase of 5.5%. In the electrical industry, the substantial usage of MMC from 1.3 million kilograms in 2007 to 1.4 million kilograms in 2008 with a predicted demand of 2.1 million kilograms in 2013 clearly indicates the rising demand. Moreover, usage of aluminium composites in place of steels for making of car elements reduces not only the masses of the parts but also the total car mass. Simultaneously, the increase in fuel prices within the global market also triggered an increase of the applications of aluminium and its composites rather than steels. The decrease of vehicle mass ensued in a drop of fuel consumption by 5 to 7%.

The compositional variance depicted in Table 1 provides a clear idea of the constituent alloying elements present in the LM6 base alloy. Consequently, the undeniably excellent properties of high hardness and wear resistance supported the decision to opt for SiC [28] as the reinforcement particulates. Furthermore, as stated above, the primary goal of the present study was to explore the possibility of fabricating an alternative brake pad material. Hence, in order to cater to the demands of high strength and abrasion resistance of a braking system, it is essential to ensure the formation of a strong reinforcement-matrix bond [29]. The wettability of the base matrix plays a crucial role in enhancing the strength of the bond between the reinforcements and matrix. With the inherent wettability between LM6 matrix and SiC reinforcements not being sufficient, studies illustrated the addition of a master alloy to elevate the wettability of the base matrix [30]. Moreover, the master alloy dissolves much quicker even at lower temperatures, saving valuable energy and production time.

Table 1. Compositional variation of LM6 alloy.

Element	Al	Cu	Mg	Si	Fe	Mn	Ni	Zn	Lead	Tin	Titanium	Other
Weight%	86	0.11	0.13	11.5	0.72	0.49	0.1	0.1	0.1	0.04	0.19	0.18

As for the quantitative details, a net weight of 1200 g of MMC was fabricated from the aforementioned constituents. The relevant calculations were made in accordance to the intended final weight of the MMC with 7 wt% of SiC as reinforcements and 2 wt% of Mg addition through the master alloy to the LM6 base alloy. Such choices for the quantities of the aforementioned constituent materials were made according to the conclusions obtained from a similar study [31] by one of the co-authors that succeeded in demonstrating that the SiC addition beyond the limit of 7 wt% might lead to degradation of its tribological performances. Consequently, a net weight of 996 g of LM6 alloy, 84 g of SiC particulates, and 120g of master alloy (for 2 wt% Mg addition) was used for the fabrication process.

2.2. Methods

There are several fabrication procedures for hypereutectic Al-Si alloys and composites, each with their advantages and disadvantages. Next to gravity and conventional casting, centrifugal and stir casting are commonly used fabrication approaches for hypereutectic Al-Si alloys [32]. In general, for all fabrication methods, higher amounts of Si result in an increase in the size of primary Si and an increase in hardness. In comparison to conventional casting, stir-casted samples produce a better microstructure. Heat treatments cause a decrease in the size of primary Si and a consequent alteration of the material, whereas the addition of the right amount of reinforcement/modifier/refiner can alter material properties; moreover, with the addition of reinforcement/modifier/refiner, hardness increases, resulting in lower CoF and wear rate.

The bottom pour stir casting technique was specifically selected for the fabrication of the MMC, owing to its high-cost effectivity [33] and the unique advantage of being able to efficiently mix the reinforcements in the base metal and pour it into the mould with ease without loss at the melting temperature [34], ensuring superior distribution of the reinforcement particles into the base matrix. The whole procedure was initiated through the addition of the LM6 alloy and master alloy in a graphite crucible to be heated at a temperature of 750 °C for a net period of one hour to completely melt the constituents. At the same time, the SiC reinforcements were preheated at 550 °C in a separate crucible with the intention to prevent the formation of an oxidation layer [35] and improve wettability. The melt stirring was conducted in a setup as represented in Figure 1, where the preheated SiC reinforcements were introduced to the melt immediately with a variable stirring speed of 250 rpm to 350 rpm over a total time period of 5 min in an atmosphere of Argon gas to prevent the introduction of porosity. The bottom pour technique was then implemented to

transfer the fabricated MMC melt to a casting mould preheated at a temperature of 350 °C to conclude the fabrication process.

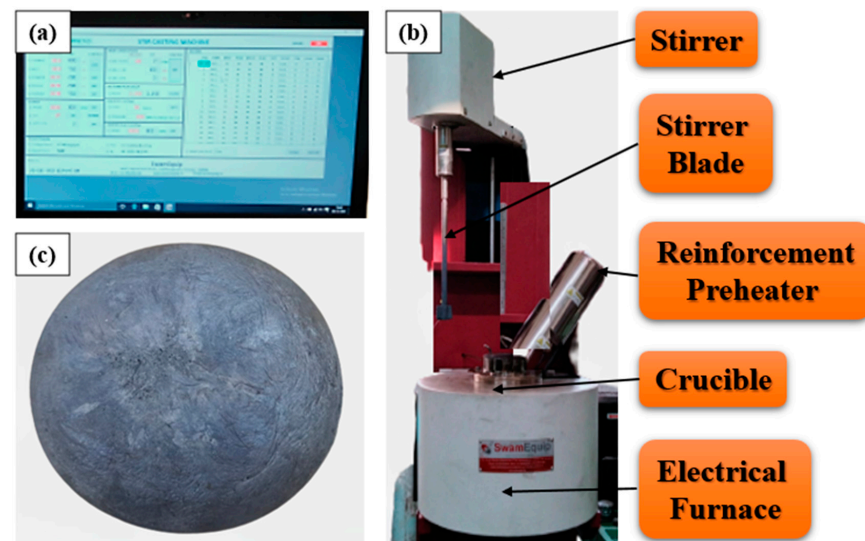


Figure 1. Schematic representation of the experimental arrangement for the stir casting process: (a) control section, (b) stir casting machine, and (c) prepared sample.

2.2.1. Energy Dispersive Spectroscopy and X-ray Diffraction Analysis

Prior to the estimation of surface hardness and tribological behaviour, the morphological investigations were conducted through optical micrography and SEM (secondary electron micrography) analysis. Furthermore, EDS (energy dispersive spectroscopy) and XRD (X-ray diffraction) analysis were also conducted to evaluate the compositional and phase variations of the fabricated MMC. Samples were polished using emery papers of 240, 600, and 1600 grid size, followed by etching treatment with Keller's reagent before obtaining micrographs of 100X and 500X magnification from Leica DM2500M optical microscope.

For SEM and EDS analysis, samples were sectioned down to cuboidal structures with dimensions of 8 mm × 8 mm × 10 mm for investigation using Zeiss Gemini Sigma 300VP scanning electron microscope, manufactured in Jena, Germany. As for the phase analysis, Bruker D8 ADVANCE diffractometer was implemented at a scan rate of 0.02°/s and range of 10° to 100°. Rockwell Hardness testing methodology was used to evaluate the surface hardness of unreinforced LM6 and fabricated MMC under a load of 100 Kgf for a net dwell time of 15 s with 1/16" tungsten carbide ball. Similarly, characterization of the material at elevated temperature was also necessary to predict the behaviour of the fabricated composite under the influence of frictional heat.

2.2.2. Thermal Conductivity Analysis

Studies [36,37] suggested the temperature of 175 °C to be suitable for the approximate temperature achieved in response to the braking action of the pad materials. Hence, the thermal conductivity analysis was also performed using NETZSCH LFA-467 hyper flash in a range between 20 °C and 175 °C to simulate conditions between ambient conditions to expected temperature of frictional heat in a braking system.

2.2.3. Tribological Analysis

Consequently, the tribological analysis was also conducted at room temperature as well as at 175 °C to precisely observe the wear resistance of the fabricated MMC in comparison to the unreinforced base alloy. For this purpose, DUOCOM ball-on-disc tribometer was used with stainless steel balls as counter body, a sliding velocity of 0.5 m/s, and a net load of 10 N. Coefficient of friction (CoF) was obtained as the raw data, and specific wear rates

for each specimen were calculated using the standard formula [38] to truly estimate the effective levels of wear resistance.

2.2.4. Scanning Electron Microscopy and Energy Dispersive X-ray Spectroscopy Analysis

Furthermore, SEM and EDS analysis were also conducted on the specimens undergoing tribological investigations after the commencement of the wear tests to obtain further information through microstructural and compositional characterization. The qualitative study of the microstructure was carried out using back scattered electron image mode.

3. Results and Discussions

3.1. Microstructural Characterization of Fabricated MMC

Although phase characterization techniques can be considered suitable to provide in-depth microstructural analysis, a preliminary investigation of the optical micrographs can prove to be necessary for correlating the mechanical behaviour of the material with its microstructure. In the present study, optical micrograph analysis of both the fabricated MMC and the unreinforced LM6 base alloy are presented in Figure 2. Careful observations of the optical micrograph of the as-cast LM6 base alloy represented in Figure 2a reveal a close resemblance of the morphological arrangements with the microstructure of Al-Si alloys going through hypoeutectic transformation [39] (less than 12 wt% of Si). The reliability of this observation can be easily braced by the information presented in Table 1, which represents the compositional variation of the constituent elements of LM6 alloy and indicates the presence of 11.5 wt% of Si. From the Al-Si phase diagram [40] presented in Figure 3, it can be noted that the present case deals with the hyper-eutectic transformation of Al-Si alloy, establishing a good agreement with the micrographic observations.

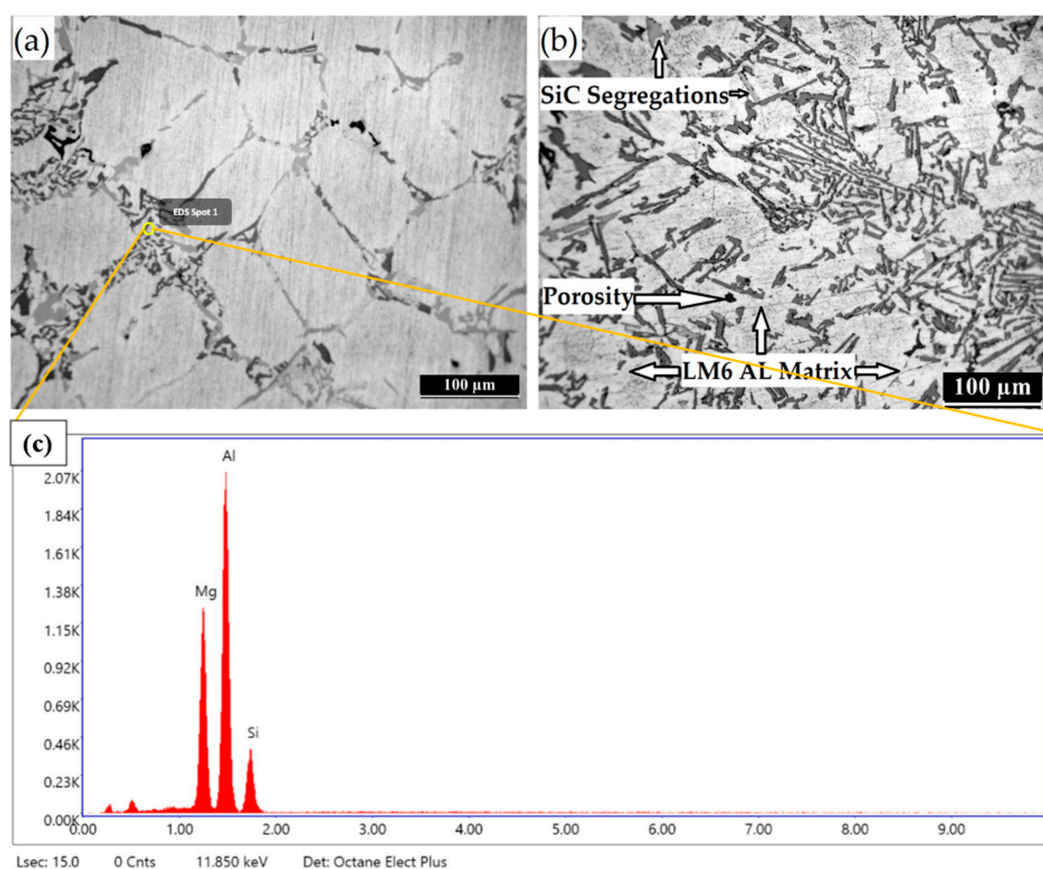


Figure 2. Optical Microscopy Micrograph of (a) LM6 base alloy at 200x (b) MMC at 200x; and (c) corresponding EDS spot analysis LM6 base alloy.

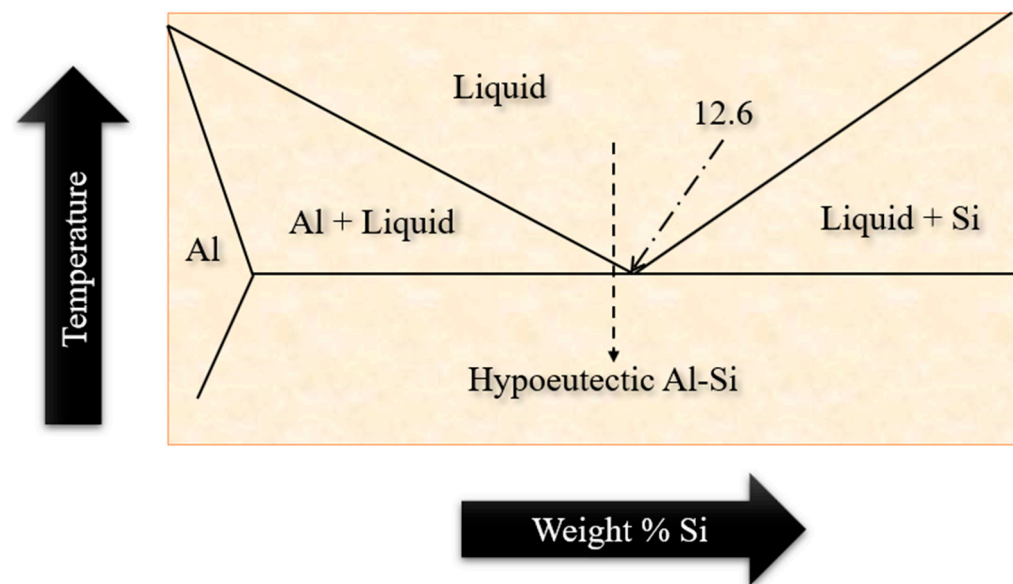


Figure 3. Al-Si phase diagram.

As for the fabricated MMC, preliminary observations reveal long segregations of SiC reinforcements, even though it was added in particulate form during the fabrication process through stir casting methodology. This behaviour can be corroborated to the non-wettability between the SiC and LM6 base matrix, since a higher surface area leads to higher wettability, as well as the influence of casting parameters implemented during the fabrication of MMC. Though the preheating process was applied prior to the stir casting of the MMC to prevent the reactions at the matrix-reinforcement interface, it also ensures a significant decline in the formation of porosity through the entrapment of air [41]. However, the optical micrograph of the fabricated MMC displays minimal presence of porosity as well.

3.2. Compositional and Phase Analysis of Fabricated MMC through SEM, EDS, and XRD

The EDS analysis of the fabricated MMC was obtained with the intention of accurately estimating the compositional variation and distribution. Furthermore, EDS analysis lays down the foundation to conduct the investigation on detecting the elements present, which can further be confirmed by the successful analysis of XRD peaks. The EDS spot analysis as shown in Figure 4 displays an expected behaviour, with the EDS peak represented in Figure 4b with a darker grey tone in colour revealing high peaks of Al, Si, and C; this indicates the morphological feature to be SiC reinforcements. Similarly, the second spot analysis displayed in Figure 4c indicates one considerably high peak for Al, evidencing the morphological feature with light grey tone to be the LM6 base alloy matrix. A more precise quantitative analysis was obtained from the EDS map analysis and is presented in Figure 5a, where the elemental distribution is revealed in terms of comparative weight percentages. Apart from the expected high weight percentage of Al and Si, the presence of Mg was also detected, which can be explained by the addition of the master alloy, as mentioned in the fabrication procedure in the “Materials and Methods” section.

An EDS line scan conducted in a similar microstructural area of spot analysis confirmed the preliminary assumptions made from the EDS spot investigations as represented in Figure 5c. The decline in the graph representing Si wt% as one moves along the line from left to right indicates the credibility of the statement that the morphological features of a darker grey colour are SiC reinforcements, whereas the light grey colour represents the LM6 base matrix.

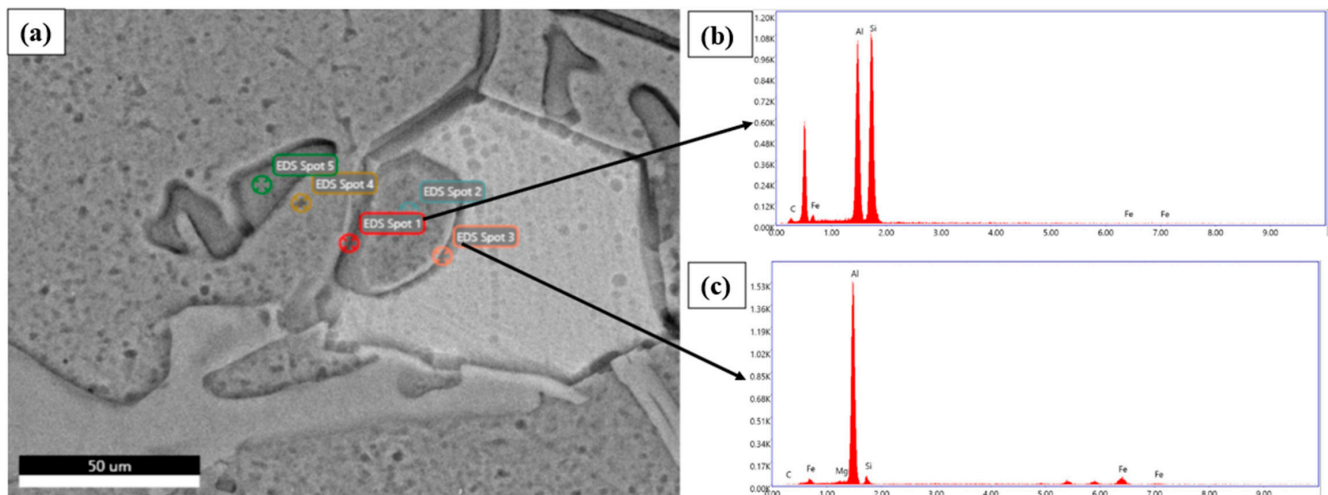


Figure 4. (a) SEM-BES morphology of MMC and EDS spectra of (b) SiC reinforcement and (c) LM6 base matrix.

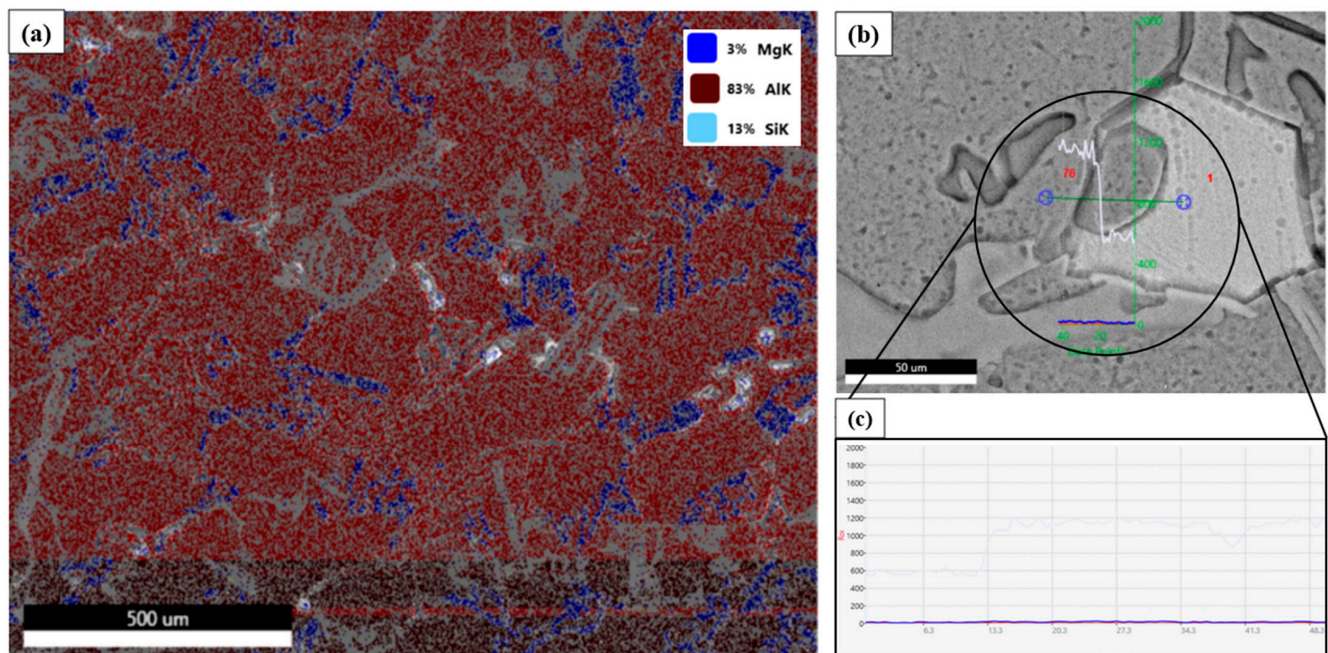


Figure 5. EDS analysis of fabricated MMC in (a) map of Mg, Al, and Si content and (b) line-scan method representing Si content.

Although a primary idea of the compositional variation was sufficiently acquired from the EDS analysis, the precise estimations of phases present and their crystallographic orientations were obtained through XRD analysis with references from JCPDS XRD database. Figure 6 representing the XRD peaks reveals the occurrence of Al oriented along (111), (002), (022), and (222), which is expected due to the wide presence of the LM6 base alloy matrix. Consequently, the existence of Si peaks along the planes of (220), (311), (331), and (442) reaffirms the major alloying wt% of Si in LM6 alloy matrix. Furthermore, SiC peaks also appeared in the XRD analysis aligned along the planes of (111) and (002), signifying the successful incorporation of the reinforcements in the LM6 base alloy matrix.

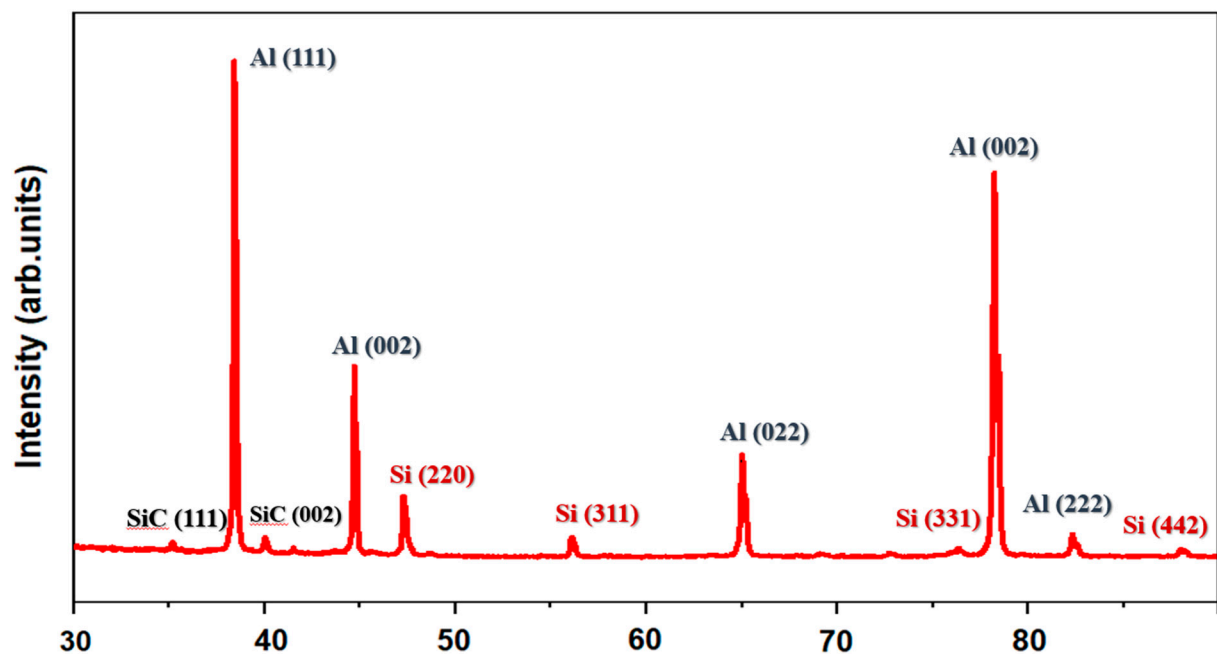


Figure 6. XRD spectrum of fabricated MMC.

Contrary to the behaviour of the fibre-reinforced composites that distinctly display the influence of fibre orientation on the mechanical properties of the base matrix, the particulate distribution in the present study does not reveal such significant effects of reinforcement orientation [42]. Furthermore, the presence of the Mg added through the master alloy was once again detected from the XRD peak analysis that revealed Mg preferentially aligned along the (020) plane. One of the most noticeable traits of the fabricated MMC was the absence of Al_4C_3 in both the EDS and XRD analysis, even though multiple studies of a similar nature revealed its undesirable presence [43]. This appreciable behaviour can be corroborated by the optimized process parameters [44] applied for the casting methodology in the present fabrication process in accordance to several studies that indicate the recommended parameters necessary to avoid the undesirable formation of the brittle carbides [45]. On the outset, the EDS and XRD analysis indicated a good agreement of results between the conclusions drawn from the investigations.

3.3. Rockwell Hardness Analysis of Fabricated MMC

Surface hardness estimations are the best option for the successful characterization of the surface strength of Al-SiC composites [46]. For the successful implication as brake pad material, it is necessary for the fabricated MMC to bear considerably high surface hardness. Rockwell hardness conducted on unreinforced base alloy as well as the fabricated MMC under the implementation of 100 Kgf through 1/16" tungsten carbide ball revealed the trends of surface hardness. Expectedly, the introduction of SiC as reinforcements in the soft base matrix of LM6 alloy led to the increment in surface hardness values from about 47.3 HRB in case of the base alloy to 68.3 HRB for the MMC. The presence of the second phase in form of SiC particles provide a localized hindrance to the dislocation movement, resulting in increased surface hardness. Furthermore, as dictated by the Orowan's mechanism [47] of dispersion hardening, it can be predicted that the hard SiC phases present in the LM6 base matrix will make the advancing dislocation line bow around [48] rather than cut through. This consequently leads to the formation of dislocation loops [49] around the SiC particulates, which further resists the movements of incoming dislocations.

Moreover, it is equally necessary to view the reinforcement-matrix interface interaction from an atomic level in order to truly explain the significant increase in surface hardness upon reinforcing SiC on LM6. Owing to the considerably low wettability between the SiC

and LM6 base matrix, mechanical bonding at the matrix-reinforcement interface cannot be expected to be extensive enough through the interlocking mechanism [50]. However, it is also essential to reiterate that the absence of the formation of Al_4C_3 , which is a diffusion reaction product [51], indicates the lack of interfacial reactions through diffusion bonding between the SiC reinforcements and LM6 base alloy matrix. Hence, the overall interfacial strength to resist the dislocation mobility can be associated to the nature of the reinforcement-matrix bonding, which is an intermediate between diffusion and mechanical interlocking.

The obtained values of hardness analysis also revealed acceptable levels of surface hardness necessary for its application as a brake pad material [52]. Even though the addition of SiC reinforcements beyond 7 wt% would surely elevate the surface hardness, the corresponding deterioration in tribological performance as suggested by similar studies [53] was considered as a standard for determining the upper limit of SiC addition in the formulation of the brake pad material.

3.4. Thermal Conductivity Analysis of the Fabricated Composite

Although the mechanical strength for the use of the fabricated MMC as a brake pad material can be estimated precisely through the surface hardness evaluation, it is equally necessary to investigate the thermal behaviour of the material. Since it is impossible to ignore the inevitable effects of heat evolved owing to the frictional behaviour of the braking system, the thermal conductivity evaluation was deemed as a necessary characterization process for determining the possibility of using the fabricated MMC as a novel brake pad material. The thermal conductivity of a brake pad material plays an immensely crucial role in determining the efficacy of the braking system, given the need for the proper dissipation of the heat generated through the transformation of kinetic energy to thermal energy owing to the friction between the brake pad surfaces [54].

The utmost importance of considering materials with high thermal conductivity as material in brake pads has been separately dealt with in several studies [55]. Furthermore, the tribological performance of a composite is also expected to improve significantly [56] in the case of aluminium matrix composites with higher thermal conductivity, which prominently displays the importance of having appreciable thermal conductivity for brake pad materials.

As represented in Figure 7, the fabricated MMC revealed an appreciable increase in thermal conduction and diffusivity in comparison to the unreinforced base alloy, making it a suitable candidate for brake pad material. Both higher conductivity and diffusivity indicates that the fabricated MMC is perfectly capable of ensuring the proper dissipation of heat energy accumulated from the frictional effect of the braking system. The influence of reinforcement size in determining the thermal conductivity of the fabricated MMC has been vividly discussed in earlier investigations [57,58] that show how an increase in reinforcement size leads to an elevation in thermal conductivity of a composite with a constant wt% of SiC.

3.5. Tribological Behaviour of Fabricated Composite at Varied Temperatures

For the estimation of reliability as a brake pad material, the surface behaviour of the fabricated MMC should be subjected to extensive scrutiny. Although the surface hardness analysis was sufficient to indicate the durability of the fabricated MMC in comparison to the presently accepted standards of a brake pad, it is equally essential to investigate the tribological behaviour to precisely quantify the ability to resist wear. Although, thermal conductivity analysis established the ability of the composite to successfully dissipate the heat evolved due to the frictional action of the disc brake system, the tribological tests in the present study were conducted both at room temperature as well as elevated temperature. With the intention to simulate the practical conditions as perfectly as possible, the elevated temperature was set at 175 °C in reference to the temperature evolved at on a disc brake from the standard data available. After the completion of the tribological examinations, the

specific wear rate was evaluated in accordance to the Archard's equation to estimate the wear resistance perfectly.

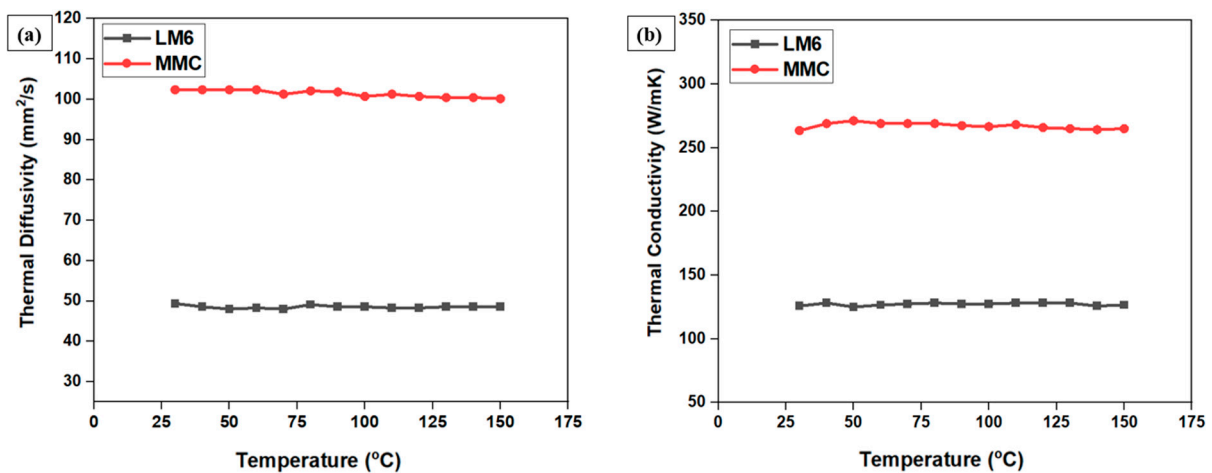


Figure 7. Comparative plots of (a) thermal diffusivity and (b) thermal conductivity of LM6 base alloy and fabricated MMC.

It has been well established that the CoF is a tribological property and not a material property that solely depends upon the behaviour of two surfaces in contact [59]. However, in the present investigation, Figure 8a reveals an initial increment in the CoF values, after which it somewhat achieves a constancy in magnitude in the case of room temperature wear tests for both LM6 and MMC. For unreinforced LM6 base alloy, this behaviour can be corroborated to the surface roughness decreasing through the plastic deformation of the base matrix resulting from the constant grinding of the surfaces in contact during the tribological tests.

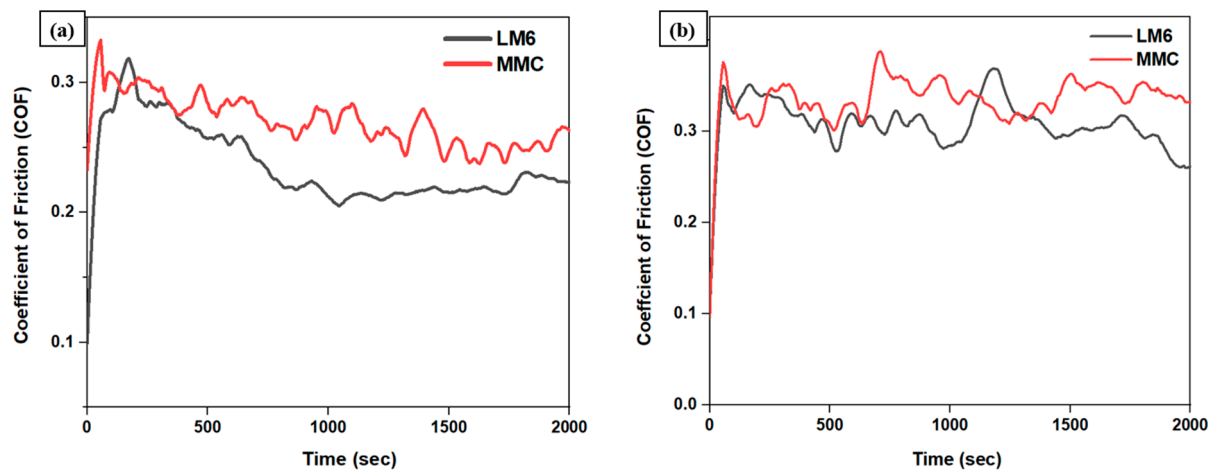


Figure 8. Comparative CoF plots of LM6 and MMC at (a) room temperature and (b) elevated temperature of 175 °C.

In case of the fabricated MMC, the hard SiC particles that contribute to the initial high CoF of the MMC surface are displaced gradually over the soft LM6 base matrix, which leads to a decrease in CoF values over time [60]. However, in the case of wear tests conducted at 175 °C, a plateau of CoF values was not observed with the increase in time, as represented in Figure 8b, which is in perfect agreement to one of the studies conducted previously on evaluating the effect of temperature on wear behaviour [61]. The study concluded that often, reinforced aluminium matrix composites suffer from excessive thermal softening

of the base matrix that concluded the formation of transfer layers of particulates to be the reason for delayed wear failure.

According to Kong et al. [62], graphite particles are exceptional self-lubrication influencers till 200 °C. Thus, it could be stated that the self-lubricating actions of graphite accounted for the prominent decline in COF value in the MMC specimen compared to LM6 at 175 °C. Contrariwise, the plastic deformations due to thermal stresses (sliding at elevated temperature) intensely affected the specific wear rate and resulting COF in the LM6 specimen against stainless steel. At higher temperatures, a great amount of grain pull out from LM6 surface by stainless steel ball occurs. Concurrently, owing to the absence of any graphite and SiC phases, the LM6 specimen experiences excessive material erosions from the surface during sliding at 175 °C. Subsequently, the highest specific wear rate and COF values were obtained for LM6 after tribological tests at 175 °C.

Upon the subsequent calculation of specific wear rate, the actual influence of reinforcing SiC particulates were revealed for both ambient and elevated temperatures. Although the LM6 samples recorded an approximate specific wear rate of $3.76 \times 10^{-4} \text{ mm}^3/\text{Nm}$ and $1.83 \times 10^{-4} \text{ mm}^3/\text{Nm}$ for room temperature and 175 °C, respectively, the SiC reinforced samples showed elevated wear resistance with a specific wear rate of $2.67 \times 10^{-4} \text{ mm}^3/\text{Nm}$ and $1.67 \times 10^{-4} \text{ mm}^3/\text{Nm}$ for ambient and elevated conditions, respectively. The increase in the wear resistance of fabricated MMCs can be reasoned with the tendency of the composite to transfer the load imposed by the steel ball from the matrix to the hard SiC phases. Furthermore, it is necessary to take into account that SiC has a higher ability to resist sub-surface shear against the steel counter body, owing to its exceptional hardness [63]. At the same time, these SiC particulates may also act as second body abrasives, increasing the wear rate of the material [64], for which an optimized quantity of SiC addition is essential. This reiterates the necessity of opting for 7 wt% addition of SiC particulates.

As for the increase in the wear rate with the increment in temperature for LM6, the onset of transition from mild to severe wear [56] due to the frictional heat reaching the critical value (0.4 time of the melting temperature of the alloy) can be considered responsible. However, in the present study, such a transition of wear magnitude is not visible from the specific wear rate values, which display a contradicting behaviour with a decline in wear rate with an increase in temperature. This can be easily explained by the fact that 175 °C is not sufficient to trigger the transition from mild to severe wear. Hence, the fabricated MMC can be considered a durable alternative to withstand the friction-induced heat generation. Furthermore, elevated temperatures might result in thermal-activated slip systems that successfully counter the effect of strain hardening caused at ambient temperatures by the action of counter body load along the wear track. This also supports the investigations surrounding the decrease in wear rate at elevated temperatures. Furthermore, the EDS analysis of the wear track of the fabricated MMC at ambient and elevated temperature presented in Figure 9 revealed the presence of a mechanical mixed layer (MML) for investigations at 175 °C.

The significant quantity of oxygen visible in the region with white morphological appearance in the EDS analysis of the samples that underwent wear tests at 175 °C indicates the presence of oxide that can be considered to be a reason to depreciate the wear loss at elevated temperature. Exposed worn surface usually experiences the formation of MML that acts as a solid lubricant and hence contributes positively towards improving the wear resistance of the fabricated MMC at elevated temperatures. Moreover, owing to the low wt% of SiC reinforcements in the present study, the MML can be considered as stable in nature for lower load applications, which explains the decline in wear rate at elevated temperatures.

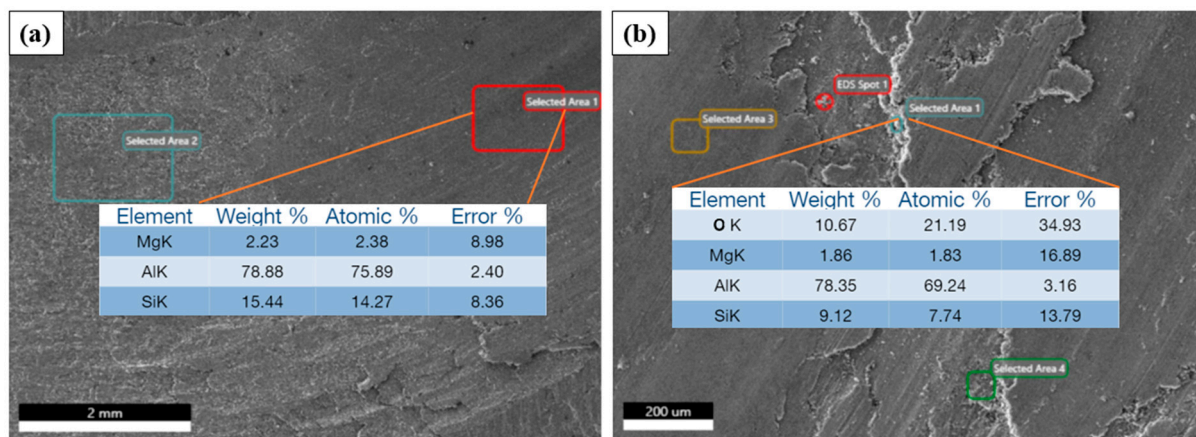


Figure 9. Comparative element weight distribution derived from EDS spot analysis on SEM images of MMC at (a) room temperature and (b) elevated temperature of 175 °C.

4. Conclusions

With the intention to replace the conventional asbestos-based brake pads, the present study focused on implementing a SiC-reinforced LM6 Aluminium alloy composite as a potential alternative. Although the particulate environmental contamination might not be as minimized as in case of organic brake pads, it does contribute in declining the quantity of wear debris in comparison to conventional brake pads, along with an optimized compilation of better surface properties than organic brake properties. All the experimental investigations conducted with a contrast to the LM6 base alloy proved the fabricated composite to bear superior mechanical and tribological properties. The detailed conclusions are listed below:

1. Owing to the high cost-effectivity, the bottom pour stir-casting methodology proved to be a more efficient process in ensuring the homogenous distribution of the SiC reinforcements. With due reference to some of the reputed works on the influence of process parameters of the casting methodology, the casting process was precisely monitored to achieve the results that were aimed for.
2. In-depth microstructural and compositional characterizations revealed the success of controlling the process parameters to effectively decrease the porosity and not only enable the uniform distribution of SiC particulates but also prevent the formation of the Al_4C_3 brittle intermetallic compound due to the negligible contact time between the matrix and reinforcement. Hence, the crucial effect of the process parameters on the microstructure of the cast cannot be neglected.
3. Surface hardness estimations revealed the significant elevation in hardness in the case of reinforced composites caused by the dislocation immobility around the hard SiC reinforcements. Moreover, the high hardness values approximately corresponded with those values that are expected from an efficient braking pad material, which highlights the success of the study.
4. Tribological investigations reaffirmed the potential of the fabricated MMC to serve as an alternative brake pad material. Especially for tests conducted at an elevated temperature of 175 °C with due consideration of the effect of heat generation from the frictional action of the brake pads, the fabricated MMCs revealed a superior wear-resisting ability. Furthermore, the visible presence of MML was also revealed through the EDS compositional analysis, which contributed significantly to the depreciation of wear loss at elevated temperatures.

Author Contributions: Conceptualization, A.C., S.S.; methodology, A.C.; software, S.S.; validation, A.C., S.S., P.R., K.D.; formal analysis, A.C., S.S.; investigation, A.C., S.P., P.R.; resources, M.G., G.S., A.H.S., I.A.A.; data curation, S.S., S.P., K.D.; writing—original draft preparation, S.S., A.C.; writing—review and editing, A.C., S.S., M.G., A.H.S., I.A.A.; visualization, A.C., G.S., M.G.; supervision, M.G.,

G.S.; project administration, G.S., M.G.; funding acquisition, A.H.S., I.A.A. All authors have read and agreed to the published version of the manuscript.

Funding: This research was funded by the Researchers Supporting Project number RSPD2023R597, King Saud University, Riyadh, Saudi Arabia.

Data Availability Statement: Data available on request due to privacy restrictions. The data presented in this study are available on request from the corresponding author. The data are not publicly available since it is intended to be further used for future experimentations by the group for upcoming projects.

Acknowledgments: The authors would like to acknowledge the Researchers Supporting Project number (RSPD2023R597), King Saud University, Riyadh, Saudi Arabia.

Conflicts of Interest: The authors declare no conflict of interest.

References

1. Ciudin, R.; Verma, P.C.; Gialanella, S.; Straffelini, G. Wear debris materials from brake systems: Environmental and health issues. *WIT Trans. Ecol. Environ.* **2014**, *191*, 1423–1434. [\[CrossRef\]](#)
2. Maiorana, S.; Teoldi, F.; Silvani, S.; Mancini, A.; Sanguineti, A.; Mariani, F.; Cella, C.; Lopez, A.; Potenza, M.A.C.; Lodi, M.; et al. Phytotoxicity of wear debris from traditional and innovative brake pads. *Environ. Int.* **2019**, *123*, 156–163. [\[CrossRef\]](#) [\[PubMed\]](#)
3. Idris, U.D.; Aigbodion, V.S.; Abubakar, I.J.; Nwoye, C.I. Eco-friendly asbestos free brake-pad: Using banana peels. *J. King Saud Univ. -Eng. Sci.* **2015**, *27*, 185–192. [\[CrossRef\]](#)
4. Mutlu, I.; Sugözü, I.; Keskin, A. The effects of porosity in friction performance of brake pad using waste tire dust. *Polímeros Ciência E Tecnologia* **2015**, *25*, 440–446. [\[CrossRef\]](#)
5. Olabisi, A.I.; Adam, A.; Okechukwu, O.A. Development and assessment of composite brake pad using pulverized cocoa beans shells filler. *Int. J. Mater. Sci. Appl.* **2016**, *5*, 66–78.
6. Kumar, N.; Natrayan, L.; Kasirajan, G.; Kaliappan, S.; Raj Kamal, M.D.; Patil, P.P.; Chewaka, M.D. Development of novel bio-mulberry-reinforced polyacrylonitrile (PAN) fibre organic brake friction composite materials. *Bioinorg. Chem. Appl.* **2022**, *2022*, 1–11. [\[CrossRef\]](#) [\[PubMed\]](#)
7. Bahari, S.A.; Isa, K.H.; Kassim, M.A.; Mohamed, Z.; Othman, E.A. Investigation on Hardness and Impact Resistance of Automotive Brake Pad Composed with Rice Husk Dust. *AIP Conf. Proc.* **2012**, *1455*, 155–161. [\[CrossRef\]](#)
8. Komai, K.; Minoshima, K.; Ryoson, H. Tensile and fatigue fracture behavior and water-environment effects in a SiC-whisker/7075-aluminum composite. *Comp. Sci. Technol.* **1993**, *46*, 59–66. [\[CrossRef\]](#)
9. Daoud, A.; Abou El-khair, M.T. Wear and friction behavior of sand cast brake rotor made of A359-20 vol% SiC particle composites sliding against automobile friction material. *Tribol. Int.* **2010**, *43*, 544–553. [\[CrossRef\]](#)
10. Fei, W.D.; Hu, M.; Yao, C.K. Effects of thermal residual stress creeping on microstructure and tensile properties of SiC whisker reinforced aluminum matrix composite. *Mater. Sci. Eng. A* **2003**, *356*, 17–22. [\[CrossRef\]](#)
11. Ghanaraja, S.; Ray, S.; Nath, S.K. Comparative Analysis of the particle size on the porosity and the tensile properties of aluminium based metal matrix nano-composites. *Mater. Today Proc.* **2021**, *46*, 9013–9020. [\[CrossRef\]](#)
12. Palanivendhan, M.; Chandaradass, J.; Philip, J. Fabrication and mechanical properties of aluminium alloy/bagasse ash composite by stir casting method. *Mater. Today Proc.* **2021**, *45*, 6547–6552. [\[CrossRef\]](#)
13. Ahmad, F.; Jason Lo, S.H.; Aslam, M.; Haziq, A. Tribology behaviour of alumina particles reinforced aluminium matrix composites and brake disc materials. *Procedia Eng.* **2013**, *68*, 674–680. [\[CrossRef\]](#)
14. Khan, M.M.; Dixit, G. Comparative study on erosive wear response of SiC reinforced and fly ash reinforced aluminium based metal matrix composite. *Mater. Today Proc.* **2017**, *4*, 10093–10098. [\[CrossRef\]](#)
15. Mahaviradhan, N.; Sivaganesan, S. Tribological analysis of hybrid aluminum matrix composites for high temperature applications. *Mater. Today Proc.* **2021**, *39*, 669–675. [\[CrossRef\]](#)
16. Govindan, K.; Elatharasan, G.; Thulasi, S.; Vijayalakshmi, P. Tensile, compressive and heat transfer analysis of ZrO₂ reinforced aluminum LM6 alloy metal matrix composites. *Mater. Today Proc.* **2021**, *37*, 303–309. [\[CrossRef\]](#)
17. Akinwamide, S.O.; Lesufi, M.; Akinribide, O.J.; Mpolo, P.; Olubambi, P.A. Evaluation of microstructural and nanomechanical performance of spark plasma sintered TiFe-SiC reinforced aluminium matrix composites. *J. Mater. Res. Technol.* **2020**, *9*, 12137–12148. [\[CrossRef\]](#)
18. Madhavarao, S.; Ramabhadri, C.R.; Madhukiran, J.; Varma, N.S.; Varma, P.R. A study of tribological behaviour of aluminum-7075/SiC metal matrix composite. *Mater. Today Proc.* **2018**, *5*, 20013–20022. [\[CrossRef\]](#)
19. Kalhapure, V.A.; Khairnar, H.P. Taguchi method optimization of operating parameters for automotive disc brake pad wear. *Appl. Eng. Lett.* **2021**, *6*, 47–53. [\[CrossRef\]](#)
20. Surappa, M.K. Aluminium matrix composites: Challenges and opportunities. *Sadhana* **2003**, *28*, 319–334. [\[CrossRef\]](#)
21. Koli, D.K.; Agnihotri, G.; Purohit, R. Advanced aluminium matrix composites: The critical need of automotive and aerospace engineering fields. *Mater. Today Proc.* **2015**, *2*, 3032–3041. [\[CrossRef\]](#)

22. Efzan, E.; Nordin, S.S.; Abdullah Al Bakri, M.M. Microstructure and mechanical properties of fly ash particulate reinforced in LM6 for energy enhancement in automotive applications. *IOP Conf. Ser. Mater. Sci. Eng.* **2016**, *133*, 012046. [\[CrossRef\]](#)
23. Chelladurai, S.J.S.; Arthanari, R. Investigation on mechanical and wear properties of zinc-coated steel wires reinforced LM6 aluminium alloy composites by squeeze casting. *Surf. Rev. Lett.* **2019**, *26*, 1850125. [\[CrossRef\]](#)
24. Chelladurai, S.J.S.; Arthanari, R.; Nithyanandam, N.; Rajendran, K.; Radhakrishnan, K.K. Investigation of mechanical properties and dry sliding wear behaviour of squeeze cast LM6 aluminium alloy reinforced with copper coated short steel fibers. *Trans. Indian Inst. Met.* **2018**, *71*, 813–822. [\[CrossRef\]](#)
25. Shivaramu, H.T.; Umashankar, K.S.; Prashantha, D.A. Wear characteristics comparison of cast and powder metallurgy based Al and Al-Si alloy [LM6]. *Mater. Today Proc.* **2018**, *5*, 8138–8146. [\[CrossRef\]](#)
26. Vignesh, R.; Gandhi, S.M.; Vignesh, A.; Rajarajan, P. Effect of squeeze cast process parameters on fluidity of aluminium LM6 alloy. *Int. J. Adv. Technol.* **2016**, *7*, 157. [\[CrossRef\]](#)
27. Stojanović, B.; Ivanović, L. Application of aluminium hybrid composites in automotive industry. *Tehnički Vjesnik* **2015**, *22*, 247–251. [\[CrossRef\]](#)
28. Nair, S.V.; Tien, J.K.; Bates, R.C. SiC-reinforced aluminium metal matrix composites. *Int. Met. Rev.* **1985**, *30*, 275–290. [\[CrossRef\]](#)
29. Chappell, P.J. *Reinforcement-Matrix Interface Effects in Metal Matrix Composites*; Materials Research Labs Ascot Vale: Melbourne, Victoria, Australia, 1989.
30. Prema, S.; Chandrashekharaiah, T.M.; Begum, P.F. Effect of grain refiners and/or modifiers on the microstructure and mechanical properties of Al-Si Alloy (LM6). *Mater. Sci. Forum.* **2019**, *969*, 794–799. [\[CrossRef\]](#)
31. Pradhan, S.; Barman, T.K.; Sahoo, P.; Sutradhar, G. Effect of SiC weight percentage on tribological properties of Al-SiC metal matrix composites under acid environment. *J. Tribol.* **2017**, *13*, 21–35.
32. Miladinović, S.; Stojanović, B.; Gajević, S.; Vencl, A. Hypereutectic Aluminum Alloys and Composites: A Review. *Silicon* **2022**. [\[CrossRef\]](#)
33. Hashim, J.; Looney, L.; Hashmi, M.S.J. Metal matrix composites: Production by the stir casting method. *J. Mater. Process. Technol.* **1999**, *92*, 1–7. [\[CrossRef\]](#)
34. Kumar, G.B.V.; Annigeri, U.K. Method of stir casting of aluminum metal matrix composites: A review. *Mater. Today Proc.* **2017**, *4*, 1140–1146. [\[CrossRef\]](#)
35. Almadhoni, K.; Khan, S. Review of effective parameters of stir casting process on metallurgical properties of ceramics particulate Al composites. *IOSR J. Mech. Civ. Eng.* **2015**, *12*, 22–40. [\[CrossRef\]](#)
36. Chatterjee, A.; Sen, S.; Paul, S.; Ghosh, K.; Ghosh, M.; Sutradhar, G. Fabrication and Characterization of Silicon Carbide and Graphite Reinforced Aluminium Matrix Composite. *J. Inst. Eng. India Ser. D* **2022**, 1–15. [\[CrossRef\]](#)
37. Chatterjee, A.; Sen, S.; Paul, S.; Ghosh, K.; Roy, P.; Sutradhar, G.; Ghosh, M. Application of SiC and Graphite reinforced Aluminium Metal Matrix Composite in Braking Systems and its Validation Through Finite Element Analysis. *J. Inst. Eng. India Ser. D* **2022**, 1–16. [\[CrossRef\]](#)
38. Kraghelsky, I.V. Calculation of wear rate. *J. Basic Eng.* **1965**, *87*, 785–790. [\[CrossRef\]](#)
39. Saini, N.; Dwivedi, D.K.; Jain, P.K.; Singh, H. Surface modification of cast Al-17% Si alloys using friction stir processing. *Procedia Eng.* **2015**, *100*, 1522–1531. [\[CrossRef\]](#)
40. Okamoto, H.; Massalski, T.B. *Binary Alloy Phase Diagrams*; ASM International: Materials Park, OH, USA, 1990; Volume 12.
41. Sijo, M.T.; Jayadevan, K.R. Analysis of stir cast aluminium silicon carbide metal matrix composite: A comprehensive review. *Procedia Technol.* **2016**, *24*, 379–385. [\[CrossRef\]](#)
42. May, G.J. The influence of off-axis reinforcement on the tensile strength of an Ni-Al-Cr-C eutectic composite. *J. Mater. Sci.* **1975**, *10*, 77–82. [\[CrossRef\]](#)
43. Liu, J.; Zhou, B.; Xu, L.; Han, Z.; Zhou, J. Fabrication of SiC reinforced aluminium metal matrix composites through microwave sintering. *Mater. Res. Exp.* **2020**, *7*, 125101. [\[CrossRef\]](#)
44. Lin, R.Y. Interface evolution in aluminum matrix composites during fabrication. *Key Eng. Mater.* **1995**, *104*, 507–522. [\[CrossRef\]](#)
45. Lee, J.C.; Byun, J.Y.; Park, S.B.; Lee, H.I. Prediction of Si contents to suppress the formation of Al₄C₃ in the SiCp/Al composite. *Acta Mater.* **1998**, *46*, 1771–1780. [\[CrossRef\]](#)
46. Mohamed, E.A.; Churyumov, A.Y. Investigation of the microstructure and properties of Al-Si-Mg/SiC composite materials produced by solidification under pressure. *Phys. Met. Metallogr.* **2016**, *117*, 1054–1060. [\[CrossRef\]](#)
47. Misra, A.; Hirth, J.P.; Kung, H. Single-dislocation-based strengthening mechanisms in nanoscale metallic multilayers. *Philos. Mag. A* **2002**, *82*, 2935–2951. [\[CrossRef\]](#)
48. Sylvain, Q.; Monnet, G.; Benoit, D. Orowan strengthening and forest hardening superposition examined by dislocation dynamics simulations. *Acta Mater.* **2010**, *58*, 5586–5595. [\[CrossRef\]](#)
49. Bacon, D.J.; Kocks, U.F.; Scattergood, R.O. The effect of dislocation self-interaction on the Orowan stress. *Philos. Mag.* **1973**, *28*, 1241–1263. [\[CrossRef\]](#)
50. Matthews, F.L.; Rawlings, R.D. Composite materials: Engineering and science. *Mater. Eng.* **1995**, *16*, 119–120. [\[CrossRef\]](#)
51. Suryanarayanan, K.; Praveen, R.; Raghuraman, S. Silicon Carbide Reinforced Aluminium Metal Matrix Composites for Aerospace Applications: A Literature Review. *International Journal of Innovative Research in Science. Eng. Technol.* **2013**, *2*, 6336–6344.
52. Ma, X.; Luan, C.; Fan, S.; Deng, J.; Zhang, L.; Cheng, L. Comparison of braking behaviors between iron- and copper-based powder metallurgy brake pads that used for C/C-SiC disc. *Tribol. Int.* **2021**, *154*, 106686. [\[CrossRef\]](#)

53. Patel, M.; Pardhi, B.; Pal, M.K.; Singh, M. SiC Particulate Reinforced Aluminium Metal Matrix Composite. *Adv. J. Grad. Res.* **2018**, *5*, 8–15. [\[CrossRef\]](#)
54. Breuer, B.; Bill, K.H. *Brake Technology Handbook*; SAE International: Warren, PA, USA, 2008.
55. Milenkovic, D.P.; Jovanovic, J.S.; Jankovic, S.A.; Milovanovic, D.M.; Vitosevic, D.N.; Djordjevic, V.M.; Raicevic, M.M. The influence of brake pads thermal conductivity on passenger car brake system efficiency. *Thermal Sci.* **2010**, *14*, 221–230. [\[CrossRef\]](#)
56. Zhang, J.; Alpas, A.T. Transition between mild and severe wear in aluminium alloys. *Acta Mater.* **1997**, *45*, 513–528. [\[CrossRef\]](#)
57. Sharifi, H.; Eidivandi, V.; Tayebi, M.; Khezlloo, A.; Aghaie, E. Effect of SiC particles on thermal conductivity of Al-4%Cu/SiC composites. *Heat Mass Transf.* **2017**, *53*, 3621–3627. [\[CrossRef\]](#)
58. Ashrafi, N.; Ariff, A.H.M.; Sarraf, M.; Sulaiman, S.; Hong, T.S. Microstructural, thermal, electrical, and magnetic properties of optimized Fe₃O₄-SiC hybrid nano filler reinforced aluminium matrix composite. *Mater. Chem. Phys.* **2021**, *258*, 123895. [\[CrossRef\]](#)
59. Nuruzzaman, D.M.; Chowdhury, M.A. Friction Coefficient and Wear Rate of Different Materials Sliding Against Stainless Steel. *Int. J. Surf. Eng. Interdiscip. Mater. Sci.* **2013**, *1*, 33–45. [\[CrossRef\]](#)
60. Walczak, M.; Pieniak, D.; Zwierzchowski, M. The tribological characteristics of SiC particle reinforced aluminium composites. *Arch. Civ. Mech. Eng.* **2015**, *15*, 116–123. [\[CrossRef\]](#)
61. Wilson, S.; Alpas, A.T. Effect of temperature on the sliding wear performance of Al alloys and Al matrix composites. *Wear* **1996**, *196*, 270–278. [\[CrossRef\]](#)
62. Kong, L.; Zhu, S.; Bi, Q.; Qiao, Z.; Yang, J.; Liu, W. Friction and wear behavior of self-lubricating ZrO₂(Y₂O₃)-CaF₂-Mo-graphite composite from 20 °C to 1000 °C. *Ceram. Int.* **2014**, *40*, 10787–10792. [\[CrossRef\]](#)
63. Al-Rubaie, K.; Yoshimura, H.N.S.; Biasoli de Mello, J.D. Two-body abrasive wear of Al-SiC composites. *Wear* **1999**, *33*, 444–454. [\[CrossRef\]](#)
64. Chen, R.; Iwabuchi, A.; Shimizu, T.; Shin, H.J.; Mifune, H. The sliding wear resistance behavior of NiAl and SiC particles reinforced aluminium alloy matrix composites. *Wear* **1997**, *213*, 175–184. [\[CrossRef\]](#)

Disclaimer/Publisher's Note: The statements, opinions and data contained in all publications are solely those of the individual author(s) and contributor(s) and not of MDPI and/or the editor(s). MDPI and/or the editor(s) disclaim responsibility for any injury to people or property resulting from any ideas, methods, instructions or products referred to in the content.